Mutations and the Recombination Hotspot Paradox

Francisco Úbeda[a,*], Frederic Fyon[a], Reinhard Bürger[b]

[a] *Department of Biology, Royal Holloway University of London, Egham TW20 0EX, UK*
[b] *Faculty of Mathematics, University of Vienna, 1090 Vienna, Austria*

Abstract

Recombination concentrates in regions called recombination hotspots. In many vertebrates including humans, gene PRDM9 specifies which DNA sequences will be targets for breaks that initiate recombination. Because the sequence that breaks (allowing recombination) is converted into the sequence that does not break (preventing recombination), the latter is over-transmitted to future generations. Given their self-destructive nature, recombination hotspots should eventually become extinct in genomes they are observed. While empirical evidence shows that individual hotspots do become inactive over time (die), hotspots are abundant in many vertebrates: a contradiction called the Recombination Hotspot Paradox. What saves recombination hotspots from their foretold extinction? Here we formulate a mathematical model of the interaction among sequence specific gene conversion (PRDM9), fertility and mutation. We find that natural selection cannot stop individual hotspots from dying but can save them from extinction by driving their re-activation (resuscitation). We find that mutations are responsible for permanent and regular oscillations between hotspots and coldspots. In our model mutations balance death and resuscitation of hotspots maintaining their numbers over time. Interestingly we find that mutations are responsible for the oscillation of individual hotspots being asynchronous across the genome such that the average recombination across the genome remains constant. Our model thus explains the paradox by reconciling predictions and empirical observations. Additionally our work provides testable predictions regarding the relation between mutation and fertility with life expectancy of hotspots. From a more applied perspective our model can be calibrated against genomic data. Such calibration would enable us to better understand linkage disequilibrium between allelic markers and diseases.

Keywords: Recombination Hotspot Paradox | PRDM9 | Gene conversion | Mutation | Recombination | Limit cycles | Intragenomic conflict | Oscillations

Introduction

Recombination —the exchange of genetic material between parental chromosomes— is a fundamental biological process that is key in generating DNA variability and trading information across genomes [22, 1, 42, 32]. It has a critical impact in ecology and evolution

*Corresponding author
Email address: f.ubeda@rhul.ac.uk (Francisco Úbeda)

(selfish genes [17], genomic architecture [18], sexual reproduction [28], speciation [7] and conservation [13]), and in human disease (fertility [27, 36], cancer [15], association between genetic variants and illness [41, 40]). The impact of recombination relies not only on the intensity of recombination but also on its distribution across the genome. Contrary to prior beliefs, recombination is not uniformly distributed across the genome but concentrated in small chromosomal regions where recombination is ten to a thousand times more frequent than the genome's average; these regions are known as *recombination hotspots* [33, 3, 30, 5]. In humans, most mammals and many vertebrates, the location of recombination hotspots is determined by the preference of alleles in PRDM9 locus for binding specific DNA motifs [26, 25, 4, 9]. Henceforth we will use the term recombination hotspots to refer to these PRDM9-directed recombination hotspots.

Empirical work shows that recombination is initiated by a double-strand break [29, 16, 33] and results in the conversion of the allele that breaks (*enabling recombination*) into the allele that does not break (*disabling recombination*) [33, 19, 20, 5]. The mechanism that initiates recombination provides an advantage in transmission to the allele disabling recombination over the allele enabling recombination [33, 19, 20, 5]. It is thus a matter of time that recombination hotspots become chromosomal regions where recombination is as frequent as the average across the genome [6] (henceforth *recombination coldspots*). This loss of activity is often referred to as the *death* of individual hotspots [10]. The self-destructive nature of recombination hotspots means that they should become extinct in genomes where they are initially found [6]. However, evidence shows that far from being rare, recombination hotspots are abundant [24, 3, 30, 5]. The *Recombination Hotspot Paradox* refers to the mismatch between the expected scarcity and observed abundance of recombination hotspots [6]: What saves recombination hotspots from their foretold extinction? Humans and chimpanzees do not share many recombination hotspots and even human subpopulations exhibit some level of recombination hotspot variation [38, 37, 48, 11, 43]. This suggests that the recombinational landscape is rapidly changing [38, 37, 48, 11, 43]. Furthermore, PRDM9 evolves extraordinarily rapidly to the point that has been considered the most rapidly evolving gene in many mammals [35]. Therefore a solution to the Recombination

Hotspots Paradox that is consistent with empirical evidence should allow for (i) individual hotspots to die, (ii) the formation of new hotspots in sufficient numbers to compensate for the lost ones, and (iii) the limited number of hotspots shared by closely related species (rapidly changing recombinational landscape).

Because recombination underpins fundamental biological processes, the Recombination Hotspot Paradox has received much attention since it was formulated [2, 34, 8, 14, 31, 47, 21, 46]. In spite of the attention received, there is no fully satisfactory solution to the paradox. The initial attempts to solve the paradox explored whether the beneficial effects of recombination on fertility —in particular how recombination favours proper chromosomal segregation during meiosis thus preventing the formation of non-viable gametes [12, 27, 39, 36]— can save recombination hotspots from extinction [6, 34, 8, 31]. Mathematical models found that the allele that does not break at the recombination hotspot (disabling recombination) spreads in the population due to its transmission advantage, even when this allele reduces the fertility of the individual carrier [6, 34, 8, 31]. To maintain the allele enabling recombination, the benefits of recombination needed to be too strong to be realistic [6, 34, 8, 31]. Furthermore, when the benefits are strong enough, natural selection prevents individual hotspots from dying which is contrary to empirical observations on the death of individual hotspots and the rapidly evolving recombinational landscape [38, 37, 48, 11, 43, 35] (Figure 1). These models, rather than solving the paradox, established that the paradox is well founded.

Advances in our understanding of the mechanisms initiating recombination found that, in many vertebrates, alleles at PRDM9 code for a protein that binds a specific sequence motif in hotspots [26, 25, 4]. Binding between protein and sequence causes a double-strand break (DSB) that initiates recombination at the binding site [25, 4]. This observation led to the verbal argument that mutations in PRDM9 could create new families of recombination hotspots that counteract the individual loss of recombination hotspots due to gene conversion [4]. A mathematical formalisation of this solution showed that fertility selection favoured alleles at the PRDM9 locus that create new families of recombination hostpots [21]. However, this work did not model the dynamics of alleles at target loci assuming

instead that mutations in PRDM9 result in fully functional recombination hotspots [21]. The dynamics of alleles at PRDM9 can not be decoupled from the dynamics of alleles at its target sites, as it is their co-evolution that determines whether target sites will be fully functional recombination hotspots or not [47, 46]. It is thus necessary to model the co-evolutionary dynamics between PRDM9 and target sites to evaluate this solution. These dynamics are complex and while in some cases they can result in the initial formation of fully functional recombination hotpots in other it does not, leading instead to the formation of sites where recombination is mild and constant (immune to the action of gene conversion) [46]. In addition, this solution requires the continuous exploration of new chromosomal targets incurring in the potential fitness cost of causing a double strand break in functional genes needs to solve the problem of requiring an infinite supply of target sites (Figure 1).

A recent solution argued that when a hotspot has its binding motif replaced by a non-binding motif due to gene conversion, natural selection for the beneficial effects of recombination favours the spread of a mutant allele at PRDM9 that binds precisely the non-binding motif at the same recombination site [46]. A mathematical model of the co-evolutionary dynamics between PRDM9 and a target site, showed that when the benefits of recombination are weak enough, natural selection favours the re-initiation of recombinational activity in the same chromosomal region where recombinational activity ceased due to conversion (*resuscitation* of a hotspot) [46]. By using the same tried and tested recombination sites over and over, this explanation avoids the potential cost of disrupting functional genes and avoids the problem of an infinite supply of target sites. However, this explanation is not fully satisfactory either. This model finds that the expected life of a hotspot increases over time and eventually, in practical terms, hotspots no longer die [46]. This is contrary to empirical observations on the death of individual hotspots and the rapidly changing recombinational landscape [38, 37, 48, 11, 43, 35] (Figure 1).

Here we explore the role of mutations in solving the recombination hotspots paradox. The most recent solution [46] did not model recurrent mutations. We formulate a deterministic mathematical model for the co-evolution between allelic sequences at PRDM9 that produce a protein binding a specific sequence motif at target sites. This model captures

that action of gene conversion, fertility selection and recurrent mutations. We find that mutations change significantly the co-evolutionary dynamics driving permanent and regular oscillations between high recombination and low recombination in the same target sites. Mutations prevent the system from getting stuck in hotspots or coldspots, a behaviour that proved to be problematic in previous explanations [46]. Thus our model provides a solution to the Recombination Hotspot Paradox that fully reconciles predictions and empirical observations. In addition, we extend our model to consider the co-evolution between PRDM9 and multiple target sites. Unexpectedly, we find that mutations drive the alternation of target sites in their oscillation between high and low recombination. The outcome is that the average recombination across the genome remains constant while the recombination in each site oscillates widely. Finally, we extend our model to consider finite populations thus bridging the gap between deterministic predictions and stochastic observations. We find that by considering finite populations the roles of conversion, fertility, and mutation does not change qualitatively. From a more applied perspective, these results allow us to predict how the expected lifetime of recombination hotspots change with mutation rates or fertility selection. Our model can be calibrated against genomic data and help understanding the association between allelic markers and disease in human subpopulations.

Methods

We model the interaction between one locus (the *modifier* locus) coding for a protein that recognizes specific motifs at one or more loci (the *target* loci) where crossover may be initiated. This is the behavior of gene PRDM9 controlling recombination hotspots in humans and many vertebrates [25, 4, 5, 9]. We start by presenting a deterministic two-allele version of the model with one modifier and one target locus. It describes the change in gamete frequencies under fertility selection, recombination, and mutation in a sufficiently large population. In Section 1 of the SM we introduce a generalised multi-allelic version from which we derive the simpler di-allelic case presented in the main text. Then we extend the deterministic model to two target loci, i.e., a three-locus two-allele model. Finally, we formulate a model assuming that the population is finite and that there may be any number

of target loci. Throughout, we assume a randomly mating diploid population with non-overlapping generations.

Deterministic one-target model

We model a modifier locus A that carries two alleles A_1 or A_2, each encoding a protein that attempts to bind a motif at a target locus B. The target locus B also carries two alleles B_1 or B_2, each corresponding to a base pair motif that the protein produced by locus A may attempt to bind. Let x_1, x_2, x_3, x_4 be the frequencies of the gametes A_1B_1, A_1B_2, A_2B_1, A_2B_2, respectively. We denote the recombination probability between modifier and target locus by r_m. For the derivation of our results we assume $r_m = \frac{1}{2}$, i.e., modifier and target locus are either far apart on the same chromosome or on separate chromosomes. This assumption is consistent with empirical observations and previous work on the topic [31, 46].

Random union of gametes results in diploid individuals whose genotype determines the outcome of meiosis in adults. We assume that alleles are equally likely to be expressed in each of the loci. As a result, each allele at the modifier locus is equally likely to produce the protein that will attempt to bind one of the two target motifs at random. We assume further that at most one binding attempt can occur per individual per generation during meiosis. We also assume that a match between subscripts of the alleles expressed at the modifier and target loci represents a match between recognition and target sequences. Thus a match between subscripts results in a DSB with probability b (where $0 < b < 1$). A mismatch between subscripts yields no DSBs. Notice that two of the gametic types, A_1B_1 and A_2B_2, produce a protein that can bind the target (crossover enabling types), whereas the other two, A_1B_2 and A_2B_1, produce a protein that cannot bind the target (crossover disabling types).

During the DSB repair process there might be a crossover event in or near the target locus with probability r_t (henceforth crossover probability) and none with probability $1-r_t$ (where $0 < r_t < 1$) [23, 33]. During the repair process the allelic motif that breaks is converted into the allelic motif that does not break with probability c and is restored to the allelic motif that breaks with probability $1 - c$ (where $0 < c < 1$) [45, 44, 23, 33]. Notice

that biased gene conversion results in the over-transmission of the allele that is less likely to break [6, 33].

Consistently with empirical observations and previous work, we assume that individuals undergoing crossover at the target locus have proper chromosomal segregation and do not suffer any fertility cost [12, 27, 39, 36, 6, 34, 31, 46]. Individuals that do not undergo crossover have defective chromosomal segregation producing non-viable gametes with probability f (where $0 < f < 1$). Alleles at the modifier locus mutate from A_1 to A_2 or vice versa with probability μ_A. Similarly, alleles at the target locus mutate from B_1 to B_2 or vice versa with probability μ_B.

Gametic types segregate following Mendelian rules which brings us back to the beginning of the census. We write $\mathbf{x} = (x_j)$ and $\mathbf{x}' = (x'_j)$ for the vectors that contain the four gametic frequencies in successive generations, $D = x_1x_4 - x_2x_3$ for the linkage disequilibrium, and $\mathbf{d} = (1, -1, -1, 1)^\top$ for the vector of signs of the linkage disequilibrium terms. We use $^\top$ for matrix or vector transposition. The 4×4 matrices $\mathbf{W} = (w_{ij})$ and $\mathbf{M} = (m_{ij})$ contain the fitnesses and the mutation probabilities, respectively, of each gametic type. The fitness matrix combines the effects of fertility selection and conversion:

$$\mathbf{W} = \big(\underbrace{\mathbf{U} - f\overbrace{(\mathbf{U} - \mathbf{B})}^{no\,break}}_{fertility} + \underbrace{\mathbf{C} \circ \overbrace{\mathbf{B}}^{break}}_{conversion}\big), \tag{1}$$

where $\mathbf{U}$ is a 4×4 matrix of ones,

$$\mathbf{B} = b \begin{pmatrix} 1 & \frac{1}{2} & \frac{1}{2} & \frac{1}{2} \\ \frac{1}{2} & 0 & \frac{1}{2} & \frac{1}{2} \\ \frac{1}{2} & \frac{1}{2} & 0 & \frac{1}{2} \\ \frac{1}{2} & \frac{1}{2} & \frac{1}{2} & 1 \end{pmatrix} \tag{2}$$

contains the break probabilities,

$$\mathbf{C} = c \begin{pmatrix} 0 & -\frac{1}{2} & 0 & 0 \\ \frac{1}{2} & 0 & 0 & 0 \\ 0 & 0 & 0 & \frac{1}{2} \\ 0 & 0 & -\frac{1}{2} & 0 \end{pmatrix} \tag{3}$$

contains the conversion probabilities, and $\circ$ denotes the pointwise (Schur) product of matrices. Finally,

$$\bar{w} = \mathbf{x}^\top \mathbf{W}\,\mathbf{x} = \tfrac{1}{2}b + (1 - \tfrac{1}{2}b)(1 - f) + \tfrac{1}{2}bf(x_1^2 + x_4^2 - x_2^2 - x_3^2) \tag{4}$$

is the population mean fitness, which is not affected by conversion.

We note the mutation matrices at the two loci:

$$\mathbf{M}_A = \begin{pmatrix} 1-\mu_A & \mu_A \\ \mu_A & 1-\mu_A \end{pmatrix} \text{ and } \mathbf{M}_B = \begin{pmatrix} 1-\mu_B & \mu_B \\ \mu_B & 1-\mu_B \end{pmatrix}. \tag{5}$$

Because mutations occur independently, the resulting gametic mutation matrix $\mathbf{M}$ is their Kronecker product, i.e., $\mathbf{M} = \mathbf{M}_A \otimes \mathbf{M}_B$.

With these ingredients, the gametic frequencies after recombination, selection, and mutation are given by

$$\mathbf{x}' = \frac{1}{\bar{w}}\mathbf{M}\big((\mathbf{W}\mathbf{x}) \circ \mathbf{x} - \mathbf{d}\,\delta D\big)\,, \tag{6}$$

where δ is a function that measures the effect of fertility and conversion on linkage disequilibrium:

$$\delta = \tfrac{1}{2}\big(\underbrace{1 - f\,\overbrace{\big(1 - \tfrac{1}{2}b\big)}^{no\,break}}_{fertility} - \underbrace{\tfrac{1}{2}c\,\overbrace{\tfrac{1}{2}b}^{break}}_{conversion}\big)\,. \tag{7}$$

For detailed derivations, see Section 1 of the SM.

The phenotype we are interested in characterising is the population mean crossover probability at the target site:

$$\bar{r}_t = \mathbf{x}^T \mathbf{B}\, r_t\, \mathbf{x} = r_t b(x_1 + x_4 - D)\,. \tag{8}$$

For simplicity, in this manuscript we assume $r_t = 1$.

Sometimes, it is more insightful to consider the allelic frequencies and the linkage disequilibrium between them, instead of the gametic frequencies. Let $p = x_1 + x_2$ and $q = x_1 + x_3$ be the frequencies of alleles A_1 and B_1 respectively (see Section 2 of the SM for details on the transformation from (x_1, x_2, x_3, x_4) to (p, q, D)).

Deterministic two-target model

In this section, we briefly outline a three-locus model that extends the previous two-locus model by adding a second locus (locus C) as potential target of the PRDM9 protein encoded by locus A. We assume that each locus can carry two alleles. We assume that during meiosis the PRDM9 protein attempts to bind one and only one target allele either at locus B or C with equal probability $\frac{1}{2}$. We continue to assume that a match between subscripts in locus A and B or C results in a DSB with probability b. All other interactions between the PRDM9 locus and its two target loci remain the same as in the previous section. Detailed equations can be found in Section 4 of the SM.

Stochastic multi-target model

In this section, we outline an stochastic version of the deterministic model introduced above to describe a populations with a finite number of individuals N that carry genomes with a variable number of target sites. We still assume that each locus can carry two alleles and that there is only one binding attempt per meiotic event. We assume that a binding may be successful if and only if the subscripts of the alleles in the PRDM9 locus and the target match. All other interactions between the PRDM9 locus and its target loci remain the same as in the original model. A detailed description of the code used in our simulations can be found in Section 5 of the SM. The code itself is available on GitHub, https://github.com/FredericFyon/Recombination-Hotspot-Unparadox.

Results

When the mutation probability is small, we find two equilibria near the corners of the state space where the frequency of one of the two crossover enabling gametic types is high and the frequency of all other gametic types is low, $\mathbf{x}^{*1}$ (close to fixation of A_1B_1) and $\mathbf{x}^{*4}$ (close to fixation of A_2B_2). We also find an internal equilibrium where all gametic types are present, $\mathbf{x}^{*5}$, and the allele frequencies p of A_1 and q of B_1 are $\frac{1}{2}$ each. The internal equilibrium exhibits substantial linkage disequilibrium (see Section 3 of the SI for explicit expressions for these equilibria).

First consider the case when the transmission gain due to fertility selection f is stronger than the transmission gain due to gene conversion $\frac{1}{2}c$, that is $f > \frac{1}{2}c$. The two equilibria near the corners, $\mathbf{x}^{*1}$ and $\mathbf{x}^{*4}$, are within the state space with biological meaning. These equilibria are stable when the mutation probability is small (Figure 2; Section 3 of the SM). The internal equilibrium, $\mathbf{x}^{*5}$, is unstable when the mutation probability is small (Figure 2; Section 3 of the SM). The linkage disequilibrium at the internal equilibrium $\mathbf{x}^{*5}$ is positive, $D^* > 0$, thus crossover enabling gametic types are over-represented at the internal equilibrium. More specifically, stronger mutation weakens linkage disequilibrium.

When $f > \frac{1}{2}c$ then the trajectories converge to one of the equilibria $\mathbf{x}^{*1}$ and $\mathbf{x}^{*4}$ and one of the crossover-enabling gametes gets nearly fixed (Figure 2). This recovers previous results indicating that when selection is unrealistically strong, it prevents the death of individual recombination hotspots and promotes a stable recombinational profile [6, 34]. Henceforth we will focus on the more realistic case when selection strength is weaker than conversion.

In the following, we consider the case when fertility selection is weaker than gene conversion, that is $f < \frac{1}{2}c$. Then the two equilibria near the corners, $\mathbf{x}^{*1}$ and $\mathbf{x}^{*4}$, are outside of the state space with biological meaning (Figure 2; Section 3 of the SM). The internal equilibrium, $\mathbf{x}^{*5}$, is stable when the mutation probability considered is small (Figure 2; see Section 3 of the SM). The linkage disequilibrium at the internal equilibrium $\mathbf{x}^{*5}$ is negative, $D^* < 0$, thus crossover disabling gametic types are over-represented at the internal equilibrium. Again, stronger mutation weakens linkage disequilibrium, i.e., it makes it less negative.

Numerical analysis shows that with fertility selection, recombination and mutation, trajectories either approach the internal equilibrium or approach a limit cycle depending on the initial conditions (Figure 2). We mapped the set of initial conditions leading to one dynamic behavior or the other using numerical methods (Figure 2). The greater the mutation probability the smaller the set of initial conditions leading to a limit cycle (Figure 2). When initially one of the gametic types is abundant and the others rare, the frequencies of the gametic types converge towards the limit cycle and oscillate regularly over time (Figure 3.A). Consistently with previous results, in the absence of mutations in the PRDM9 locus the amount of time spent in each of the corners where one gametic type is almost fixed increases in each oscillation [46] (Figure 3.B.i). Eventually the gametic frequency shows no perceptible change and the systems behaves, in practical terms, as if stuck in one of the corners (Figure 3.B.i). The introduction of mutations in the PRDM9 locus changes significantly this behavior (Figure 3.B.ii). With mutations the amount of time spent in each of the corners where one gametic type is fixed remains constant over time and the system can oscillate perpetually (Figure 3.B.ii).

The number of generations it takes for a cycle of gametic types to be completed (the *period* of the limit cycle) changes with the selection strength and the mutation probability. The closer the strength of fertility selection is to $\frac{1}{4}c$, the longer the period of the limit cycle (Figure 4.A). The greater the mutation probability, the shorter the period of the limit cycle (Figure 4.A). The period of the limit cycle is relevant because measures, indirectly, the life expectancy of recombination hotspots. The greater the period of the limit cycle the greater the life expectancy of recombination hotspots (see SM). In the absence of mutation the period increases from one oscillation to the next and it is not possible to calculate neither a period nor a life expectancy for the recombination hotspots.

The number of generations required for the replacement of one allele at the target locus (A) relative to such replacement at the modifier locus (B), depends on the selection strength and the mutation probability. When $\frac{1}{4}c < f < \frac{1}{2}c$, the replacement of alleles at the modifier locus is faster than that at the target locus (Figure 4.B.ii). When $0 < f < \frac{1}{4}c$, the replacement of alleles at locus A is slower than that at locus B (Figure 4.B.i). The closer

fertility is to $\frac{1}{4}c$, the lower the relative difference between loci in the speed of replacement of alleles. The higher the mutation probability, the lower the relative difference between loci in the speed of replacement of alleles. This difference in the speed of fixation of the alleles in PRDM9 and target loci is relevant because it would allow us to calibrate the model for the strength of fertility selection acting on recombination. In particular, a signature of stronger selective sweep in the PRDM9 locus (relative to target loci) would suggest that the fertility selection f is between $c/4$ and $c/2$. On the contrary, a signature of stronger selective sweep in the target loci (relative to the PRDM9 locus) would suggest that the fertility selection f is between 0 and $c/4$.

We extend our model to consider a second target locus in order to gain insight into the dynamics when there is more than one target (Section 4 of the SM). In particular we are interested in exploring whether the oscillation of the mean crossover probability in each target site will be maintained and if it is maintained whether both targets will be oscillating simultaneously (in *synchrony*) or not (in *asynchrony*). We show numerically that starting with populations where one gametic type is almost fixed, the system converges to a limit cycle. In this limit cycle the mean crossover probability at each target loci oscillates asynchronously while the average across target sites (*genome* mean crossover probability) remains close to constant (Figure 5.B). Notice that in the absence of mutation the mean crossover probability at each target locus oscillates in synchrony with each other and thus the genome mean crossover probability changes over time (Figure 5.A). Furthermore, the oscillations stop after a certain amount of time (as in the absence of mutations the dynamics correspond to an heteroclynic cycle).

Interestingly, we find that the mutation probability in PRDM9 and the strength of fertility selection determine the degree of asynchrony between target loci. With mutation in PRDM9 ($\mu_A > 0$), targets oscillate asynchronously with one exhibiting a high mean crossover probability when the other exhibits a low one. Because the mean crossover probability in one target compensates the mean crossover in the other one, the genome mean crossover probability remains close to constant over time. The greater the mutation probability, the greater the asynchrony in mean crossover probability between target sites and the

lower the variation in mean crossover probability in the genome (Figure 6). The intuitive reason why is that mutation generates enough genetic variation so that fertility selection can drive the sweep of a hot allele. When the two targets are hot, conversion turns them cold. As they become colder, selection for an alternative PRDM9 allele mounts up until a selective sweep in PRDM9 happens, turning coldspots into hotspots and vice-versa. If rare PRDM9 alleles are at extremely low frequencies, for example when $\mu_A = 0$, selection must mount up considerably —the two targets need to become cold before a selective sweep that turn both of them hot is triggered (Figure 5.A). As a result, targets oscillate synchronously. In contrast, if there is some standing variation in PRDM9 due to mutation ($\mu_A > 0$), such that rare PRDM9 alleles are at low —but not extremely low frequencies—, the selective sweep will be triggered sooner. Because the frequency of hot alleles in the two targets will never be exactly the same, one of them always start to turn cold before the other one does. When the mutation rate is sufficiently high, one cold target is enough to trigger the selective sweep even when the other target is hot (Figure 5.A). As a result, the selective sweep turns the hotspot into a coldspot and the coldspot into a hotspot, with the targets oscillate asynchronously. This logic extends to the effect of fertility selection, f, on the asynchrony of the oscillations: as fertility selection increases, the selective sweep can happen without both targets being cold thus favouring asynchronous oscillations.

Finally, we formulate a model assuming that the population is finite and that there may be any number of target loci (Section 5 of the SM). We find that the behaviour of the system does not change qualitatively when considering small populations and/or more than two target loci. In particular, we show that the crossover rate in individual target sites oscillates widely while the genome's crossover rate is more stable (Figure 7). We explore differences in populations of size 5 and 10 thousand individuals ($N = 5,000$ and $N = 10,000$). We find that in both cases the crossover rate in individual target sites oscillates widely, with the turnover of hotspots accelerating as the population size increases (Figure 7). We also explored differences in genomes with two and ten target loci. We find that in both cases the crossover rate in individual target sites oscillates widely, with the turnover of hotspots decelerating as the number of target size increases (Figure 7). The reason why is that, in

finite populations, genetic drift favours the loss of rare alleles that need to be recreated again for a selective sweep to occur. As the recreation of alleles is driven by mutations (which are rare), genetic drift lengthens hot and cold phases, increasing the average period of oscillations.

Discussion

Our work provides a solution to the Recombination Hotspot Paradox by reconciling the self-destructive nature of PRDM9-directed recombination hotspots with the elevated number of such hotspots observed in various genomes [6]. Here we formulate a deterministic population genetics model for the interaction between gene conversion, fertility selection, and recurrent mutation. We find that, when fertility is weaker than conversion, mutation works together with gene conversion to favour alleles at target loci that do not bind PRDM9 (cold alleles), thus acting on the death of hotspots. Fertility selection cannot prevent the loss of abundant hot alleles. However, mutation works together with fertility selection to favour alleles at the PRDM9 locus that bind alleles previously fixed by conversion at target loci (hot alleles), thus acting on the re-activation of former hotspots (resuscitation of hotspots). Fertility selection can drive the fixation of rare hot alleles. We find that even though fertility selection is not modelled explicitly as frequency dependent, in practical terms, fertility selection (when weaker than conversion) on the interaction between specific alleles acts in a frequency dependent manner with selection being weak when hot alleles are abundant and strong when hot alleles are rare. We conclude that fertility selection can not save individual recombination hotspots from dying but can drive their resuscitation.

Showing that recombination hotspots can be born/resuscitated does not grant that they will be saved from extinction, this requires that: (i) the number of hotspots that die is the same as the number of hotspots that are resuscitated, (ii) the intensity of hotspots is neither increasing nor decreasing over time. We find that mutations are key to maintaining the intensity of recombination hotspots and balancing the death and resuscitation of hotspots to prevent their extinction. Mutations work against fertility selection to prevent the system from getting stuck in hotspots, and also they work against gene conversion to prevent the

system from getting stuck in coldspots. Contrary to previous results [46], we show that target sites oscillate between hotspots and coldspots in a regular and permanent manner (Figure 3). Thus our model does not predict the extinction of hotspots but their never-ending cycling between death and resuscitation, providing a solution to the Recombination Hotspots Paradox. Our solution is compatible with all salient features of recombination hotspots, namely the death of individual hotspots, the preservation of hotspots at the genome level, and the rapid change of the recombinational landscape (with hotspots rarely being shared between closely related species). While in our model hotspots are recycled, the location of active hotspots in a particular moment in time should be unique to each subpopulation (Figure 8).

The solution we propose here overcomes the limitations of existing explanations. Our solution does not need the strong fertility selection required by previous work [6, 34]. Previous work shows that stronger fertility selection maintains recombination hotspots by preventing their death. Weaker fertility selection however does not maintain hotspots as it fails to prevent their death and cannot drive their birth [6, 34] (Figure 1). In agreement, we find that stronger fertility prevents the death of hotspots. However, our work shows that when fertility is weaker than conversion, fertility selection fails to prevent the death of hotspots but succeeds in driving their resuscitation. For every hotspot that dies another resuscitates, and thus the the number of hotspots in the genome is kept constant. In our model, it is weaker fertility selection that maintains the number of hotspots in the genome while allowing them to die due to the frequency dependence nature of selection acting on specific targets.

Our solution accounts for the formation of a finite number of fully functional recombination hotspots that avoid the potential cost of inducing a double strand break in coding genes [4, 21] (Figure 1). Previous work argued that selection can favour alleles at the PRDM9 locus that create new families of recombination hotspots thus counteracting the individual loss of recombination hotspots due to gene conversion [4]. This work did not model the dynamics of alleles at target loci, assuming instead that mutations in PRDM9 result in fully active recombination hotspots [4, 21]. However, the dynamics of alleles at PRDM9

loci can not be decoupled from the dynamics of alleles at target sites [46]. Our work shows that the birth of recombination hotspots at new target sites requires limited allelic variation in those sites. This limited allelic variation is not granted in new target sites as they evolved in a neutral manner but is granted in target sites that were former hotspots as the recombination-disabling target sequence is quickly driven to fixation. We show that due to the action of gene conversion former hotspots are pre-adapted for the activation of hotspots, and resuscitation of hotspots is more likely than the birth of new targets. In addition, the New Targets Hypothesis does not account for the potential cost of causing a double-strand break in a coding region with the inherent risk of disrupting functional genes. Our solution does not incur in this cost as PRDM9 alleles acting on costly targets are culled from the population and only tried-and-tested target sites remain part of the recycling pool. Finally, the New Targets Hypothesis requires an infinite supply of target sites from chromosomes that have a finite number of targets. Our solution requires a limited supply of target sites as these are recycled. To summarise, our work shows that natural selection favours the death and resuscitation of the same set of recombination hotspots over and over, thus eliminating the need of an infinite supply of pre-adapted recombination sites and avoiding the risk of disrupting coding genes as required by the prevailing explanation.

In our model oscillations between hotpots and coldspots are regular and permanent. Previous work shows that in the absence of mutations hotspots die and resuscitate early on but given enough evolutionary time they stop oscillating, becoming stuck in either a hotspot or a coldspot [46] (Figure 1). Thus, previous work found the formation of permanent recombination hotspots and coldspots in the long term which is contrary to empirical observations. In our solution, oscillations are not transient but continue indefinitely. We find that recurrent mutations play a key role in maintaining oscillations over evolutionary time by acting against the attempts of fertility to remain in hotspots and the attempts of conversion to remain in coldspots. By balancing the action of fertility and conversion, mutations lead to recombination hotspots with constant expected lifetime determined by fertility, conversion and mutation.

Interestingly, we find that mutations are key in maintaining a constant recombination

rate across the genome while permitting the recombination rate in each site to oscillate widely (Figure 6). We extend our model to account for the action of PRDM9 on more than one target sites. With multiple target sites, if the oscillation in targets is such that all of them are hot or cold at the same time (oscillate synchronously) the recombination in the genome (the average across sites) oscillates with them. However, if the oscillation in targets is such that the number of targets that are hot is perfectly balanced by the cold ones (oscillate asynchronously) the recombination in the genome remains constant. We find that the greater the mutation at the PRDM9 locus the smaller the fluctuation of recombination across the genome. The greater the fertility selection the smaller the fluctuation of recombination across the genome. The intuitive reason is that the recombination rate in one site conditions the strength of selection in the other sites. The more recombination coldspots, the greater the strength of fertility selection necessary to resuscitate other hotspots. The greater the availability of matching PRDM9 mutants the smaller the strength of fertility selection necessary to resuscitate other hotspots. Therefore, with lower mutation probability and/or fertility cost all target sites need to be cold before selection favours a switch resulting in all of them being hot (synchronous oscillation). With higher mutation probability and/or fertility cost some target sites need to be cold before selection favours a switch resulting in some of them being hot while the other become cold (asynchronous oscillation). In the absence of mutation all target loci oscillate synchronously and the recombination rate in the genome oscillates widely.

Our model establishes a relation between the life expectancy of recombination hotspots, mutation and fertility. Previous results find oscillations of recombination hotspots with ever increasing hot and cold phases [46]. Because in this model the duration of oscillations is always increasing it is not possible to establish the life expectancy of recombination hotspots. In our model however, the oscillation of recombination hotspots is regular, allowing us to establish their life expectancy given mutations and fertility values. Unexpectedly, we find that the life expectancy of hotspots does not always increase with the strength of fertility selection (Figure 4). In particular, assuming equal mutation rates in PRDM9 and target sites, the higher the mutation rate and the farther the strength of fertility from $\frac{c}{4}$, the

shorter the life expectancy of recombination hotspots (Figure 4). These predictions can be tested against actual data on the life expectancy of hotspots.

Our model can be calibrated against empirical data on selective sweeps in PRDM9 relative to those in recombination hotspots. Our model finds that when the strength of fertility selection exceeds one quarter of the conversion probability, $\frac{c}{2} > f > \frac{c}{4}$, target sites oscillate exhibiting gradual death of hotspots but sudden birth of hotspots (*sudden birth* dynamics) (Figure 4.B.ii). Therefore, our model predicts in that case stronger selective sweeps in genomic regions flanking PRDM9 relative to those flanking recombination hotspots. When the strength of fertility selection falls below one quarter of the conversion probability, $0 < f < \frac{c}{4}$, recombination sites oscillate with sudden death of hotspots but gradual birth of hotspots (*sudden death* dynamics) (Figure 4.B.i). Therefore, our model predicts then weaker selective sweeps in genomic regions flanking PRDM9 relative to those flanking recombination hotspots. Our work suggests the possibility of using the genetic variability in genomic regions flanking PRDM9 relative to that near recombination hotspots to calibrate the strength of fertility selection acting on human populations.

Our work clarifies the action of natural selection on the evolution of recombination hotspots showing that natural selection favors a permanent and regular oscillation between hot and cold states. The model we present here assumes a population of infinite size (deterministic model). While this assumptions is not realistic, it allows us to separate the effect of natural selection from genetic drift that are mixed in previous models [47]. In separating these effects we show that natural selection favours permanent and regular oscillations between hot and cold states in individual hotspots while maintaining constant the average recombination in the genome. To bridge the realism gap, we present a finite population (stochastic) version of our model. We find that the behaviour of the system does not change qualitatively when considering small (finite) populations. In particular, we show that the crossover rate in individual target sites oscillates widely while the genome's crossover is more stable (Figure 7).

Previous work on finite populations explores populations of small expected size ($N = 2,000$ individuals), finding that drift alone can result in the formation of hotspots [47]. The

addition of fertility selection does increase the formation of hotspots. However the turnover of hotspots is so slow that it is not possible to determine whether the intensity and number of hotspots is maintained over time or not [47]. For this same reason it is not possible to determine the life expectancy of hotspots [47]. In the finite population version of our model, we explore populations of a size similar to the expected population size in humans ($N = 5,000$ and $N = 10,000$ individuals). Here we observe clearly the turnover of hotspots with the number of hotspots being maintained on average over time. This also allows us to make predictions regarding the relation between the life expectancy of hotspots and other selective parameters opening up the possibility of calibrating the model.

To summarise, here we provide a solution to the Recombination Hotspots Paradox that is consistent with all salient empirical observations of recombination and overcomes the limitations of previous work. Turning the Recombination Hotspots Paradox into an un-paradox is a first and necessary step towards addressing the ultimate puzzle of the existence of PRDM9 directed recombination hotspots in humans. Besides offering a plausible solution to the paradox, our research offers the possibility of calibrating the model we present against genomic data. Such calibration would allow us to provide quantitative predictions of the life expectancy of hotspots given different effects of recombination on fertility. This, in turn, can be used to study the signature of oscillatory recombination hotspots on linkage disequilibrium in the mammalian genome, a pattern that is relevant to better understand links between alleles and diseases.

Acknowledgements

[FU] thanks Francisco Úbeda Tran for help resting by the Tumtum tree. [FU] and [FF] are supported by a NSFDEB-NERC Research Grant NE/T009322/1.

Author Contributions

All authors contributed equally

References

[1] Alves, I., Houle, A.A., Hussin, J.G., Awadalla, P., 2017. The impact of recombination on human mutation load and disease. Philosophical Transactions of the Royal Society B 372, 20160465.

[2] Archetti, M., 2003. A selfish origin for recombination. Journal of Theoretical Biology 223, 335–46.

[3] Arnheim, N., Calabrese, P., Tiemann-Boege, I., 2007. Mammalian meiotic recombination hot spots. Annu. Rev. Genet. 41, 369–399.

[4] Baudat, F., Buard, J., Grey, C., Fledel-Alon, A., Ober, C., Przeworski, M., Coop, G., De Massy, B., 2010. PRDM9 is a major determinant of meiotic recombination hotspots in humans and mice. Science 327, 836–840.

[5] Baudat, F., Imai, Y., De Massy, B., 2013. Meiotic recombination in mammals: localization and regulation. Nature Reviews Genetics 14, 794.

[6] Boulton, A., Myers, R.S., Redfield, R.J., 1997. The hotspot conversion paradox and the evolution of meiotic recombination. Proceedings of the National Academy of Sciences 94, 8058–8063.

[7] Butlin, R.K., 2005. Recombination and speciation. Molecular Ecology 9, 2621–2635.

[8] Calabrese, P., 2007. A population genetics model with recombination hotspots that are heterogeneous across the population. Proceedings of the National Academy of Sciences 104, 4748–4752.

[9] Cavassim, M.I.A., Baker, Z., Hoge, C., Schierup, M.H., Schumer, M., Przeworski, M., 2022. PRDM9 losses in vertebrates are coupled to those of paralogs ZCWPW1 and ZCWPW2. Proceedings of the National Academy of Sciences 119.

[10] Coop, G., Myers, S.R., 2007. Live hot, die young: transmission distortion in recombination hotspots. PLoS Genetics 3, e35.

[11] Coop, G., Wen, X., Ober, C., Pritchard, J.K., Przeworski, M., 2008. High-resolution mapping of crossovers reveals extensive variation in fine-scale recombination patterns among humans. Science 319, 1395–1398.

[12] Fledel-Alon, A., Wilson, D.J., Broman, K., Wen, X., Ober, C., Coop, G., Przeworski, M., 2009. Broad-scale recombination patterns underlying proper disjunction in humans. PLoS Genetics 5, e1000658.

[13] Frankham, R., 2005. Genetics and extinction. Biological Conservation 2, 131–140.

[14] Friberg, U., Rice, W.R., 2008. Cut thy neighbor: Cyclic birth and death of recombination hotspots via genetic conflict. Genetics August, 2229–2238.

[15] Gerton, J.L., Hawley, R.S., 2005. Homologous chromosome interactions in meiosis: diversity amidst conservation. Nature Reviews Genetics 6, 477.

[16] Goyon, C., Lichten, M., 1993. Timing of molecular events in meiosis in saccharomyces cerevisiae: stable heteroduplex dna is formed late in meiotic prophase. Molecular and Cellular Biology 1, 373—-382.

[17] Haig, D., Grafen, A., 1991. Genetic scrambling as a defence against meiotic drive. Journal of theoretical Biology 153, 531–558.

[18] Hansen, T.F., 2006. The evolution of genetic architecture. Annu. Rev. Ecol. Evol. Syst. 37, 123–157.

[19] Jeffreys, A.J., Neumann, R., 2002. Reciprocal crossover asymmetry and meiotic drive in a human recombination hot spot. Nature Genetics 31, 267–271.

[20] Jeffreys, A.J., Neumann, R., 2005. Factors influencing recombination frequency and distribution in a human meiotic crossover hotspot. Human Molecular Genetics 14, 2277–2287.

[21] Latrille, T., Duret, L., Lartillot, N., 2017. The red queen model of recombination hot-spot evolution: a theoretical investigation. Phil. Trans. R. Soc. B 372, 20160463.

[22] Lenormand, T., Engelstädter, J., Johnston, S.E., Wijnker, E., Haag, C.R., 2016. Evolutionary mysteries in meiosis. Philosophical Transactions of the Royal Society B 371, 20160001.

[23] Lichten, M., Goldman, A.S., 1995. Meiotic recombination hotspots. Annual review of genetics 29, 423–444.

[24] Myers, S., Bottolo, L., Freeman, C., McVean, G., Donnelly, P., 2005. A fine-scale map of recombination rates and hotspots across the human genome. Science 310, 321–324.

[25] Myers, S., Bowden, R., Tumian, A., Bontrop, R.E., Freeman, C., MacFie, T.S., McVean, G., Donnelly, P., 2010. Drive against hotspot motifs in primates implicates the prdm9 gene in meiotic recombination. Science 327, 876–879.

[26] Myers, S., Freeman, C., Auton, A., Donnelly, P., McVean, G., 2008. A common sequence motif associated with recombination hot spots and genome instability in humans. Nature Genetics 40, 1124–1129.

[27] Nagaoka, S.I., Hassold, T.J., Hunt, P.A., 2012. Human aneuploidy: mechanisms and new insights into an age-old problem. Nature Reviews 13, 493–504.

[28] Otto, S.P., Lenormand, T., 2002. Resolving the paradox of sex and recombination. Nature reviews, Genetics 4, 252–261.

[29] Padmore, R., Cao, L., Kleckner, N., 1991. Temporal comparison of recombination and synaptonemal complex formation during meiosis in *s. cerevisiae*. Cell 6, 1239–56.

[30] Paigen, K., Petkov, P., 2010. Mammalian recombination hot spots: properties, control and evolution. Nature Reviews Genetics 11, 221.

[31] Peters, A., 2008. A combination of cis and trans control can solve the hotspot conversion paradox. Genetics 178, 1579–1593.

[32] Petes, T.D., 2001a. Meiotic recombination hot spots and cold spots. Nature Reviews Genetics 2, 360.

[33] Petes, T.D., 2001b. Meiotic recombination hot spots and cold spots. Nature Reviews Genetics 2, 360.

[34] Pineda-Krch, M., Redfield, R., 2005. Persistence and loss of meiotic recombination hotspots. Genetics 169, 2319–2333.

[35] Ponting, C.P., 2011. What are the genomic drivers of the rapid evolution of prdm9? Trends in Genetics 5, 165–171.

[36] Powers, N.R., Dumont, B.L., Emori, C., Lawal, R.A., Brunton, C., Paigen, K., Handel, M.A., Bolcun-Filas, E., Petkov, P.M., Bhattacharyya, T., 2020. Sexual dimorphism in the meiotic requirement for prdm9: A mammalian evolutionary safeguard. Science Advances 6, eabb6606.

[37] Ptak, S.E., Hinds, D.A., Koehler, K., Nickel, B., Patil, N., Ballinger, D.G., Przeworski, M., Frazer, K.A., Pääbo, S., 2005. Fine-scale recombination patterns differ between chimpanzees and humans. Nature genetics 37, 429.

[38] Ptak, S.E., Roeder, A.D., Stephens, M., Gilad, Y., Pääbo, S., Przeworski, M., 2004. Absence of the tap2 human recombination hotspot in chimpanzees. PLoS biology 2, e155.

[39] Ren, H., Ferguson, K., Kirkpatrick, G., Vinning, T., Chow, V., Ma, S., 2016. Altered crossover distribution and frequency in spermatocytes of infertile men with azoospermia. PLoS One 11, e0156817.

[40] Rosenberg, N.A., Huang, L., Jewett, E.M., Szpiech, Z.A., Jankovic, I., Boehnke, M., 2010. Genome-wide association studies in diverse populations. Nature Reviews Genetics 11, 356.

[41] Slatkin, M., 2008. Linkage disequilibrium - understanding the evolutionary past and mapping the medical future. Nature Reviews 9, 477–485.

[42] Stapley, J., Feulner, P., Johnston, S., Santure, A., Smadja, C., 2017. Recombination:

the good, the bad and the variable. Philosophical Transactions of the Royal Society B 372, 20170279.

[43] Stevison, L.S., Woerner, A.E., Kidd, J.M., Kelley, J.L., Veeramah, K.R., McManus, K.F., Project, G.A.G., Bustamante, C.D., Hammer, M.F., Wall, J.D., 2015. The time scale of recombination rate evolution in great apes. Molecular biology and evolution 33, 928–945.

[44] Sun, H., Treco, D., Szostak, J.W., 1991. Extensive 3'-overhanging, single-stranded dna associated with the meiosis-specific double-strand breaks at the arg4 recombination initiation site. Cell 64, 1155–1161.

[45] Szostak, J.W., Orr-Weaver, T.L., Rothstein, R.J., Stahl, F.W., 1983. The double-strand-break repair model for recombination. Cell 33, 25–35.

[46] Úbeda, F., Russell, T., Jansen, V., 2019. Prdm9 and the evolution of recombination hotspots. Theoretical Population Biology 126, 19 –32.

[47] Úbeda, F., Wilkins, J.F., 2011. The red queen theory of recombination hotspots. Journal of evolutionary biology 24, 541–553.

[48] Winckler, W., Myers, S.R., Richter, D.J., Onofrio, R.C., McDonald, G.J., Bontrop, R.E., McVean, G.A., Gabriel, S.B., Reich, D., Donnelly, P., et al., 2005. Comparison of fine-scale recombination rates in humans and chimpanzees. Science 308, 107–111.

A

Recombination Hotspot Paradox	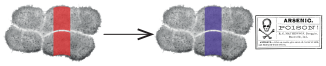	Initially: **Death** of invidual hotspots. Eventually: **Extinction** of hotspots from genome. Boulton, Myers and Redfield 1997 Pineda-Krch and Redfield 2005
Stronger Selection	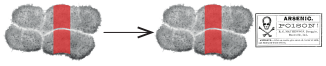	Initially and eventually: **No death** of invidual hotspots. Recombinational profile **not** rapidly **changing**. Boulton, Myers and Redfield 1997 Pineda-Krch and Redfield 2005
New Targets	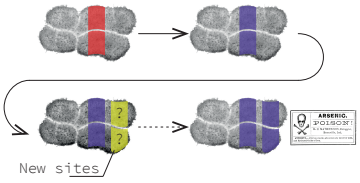	Initially: **Death** of invidual hotspots followed by birth of new hotspot? Eventually: **Extinction** of hotspots as targets either become cold or settle for mild fixed recombination Baudat et al 2010 Latrille et al 2017
Weaker Selection	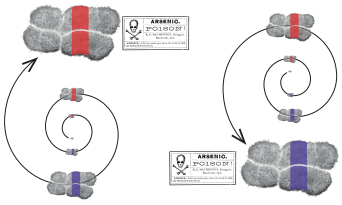	Initially: **Death** of invidual hotspots followed by resuscitation of hotspots. Recombinational profile rapidly changing. Eventually: A hotspot or a coldspot gets fixed. Recombinational profile **not** rapidly **changing**. Ubeda et al 2019

B

Mutation	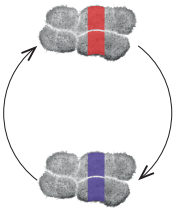	Initially and eventually: **Death** of invidual hotspots followed by resuscitation of hotspots. Rapidly **changing** recombinational profile. **Perpertual oscillation** between hotspots and coldspots.

Figure 1: **Summary of predictions of the Recombination Hotspots Paradox and its proposed solutions. Panel A** lists the paradox and its proposed solutions featuring PRDM9 trans-acting modifiers. **Panel B** corresponds to the solution we propose here. Red and blue colours represent hot and cold recombination sites. Arrows indicate changes over time. Crossbones indicate the phenotype where the evolutionary process stops.

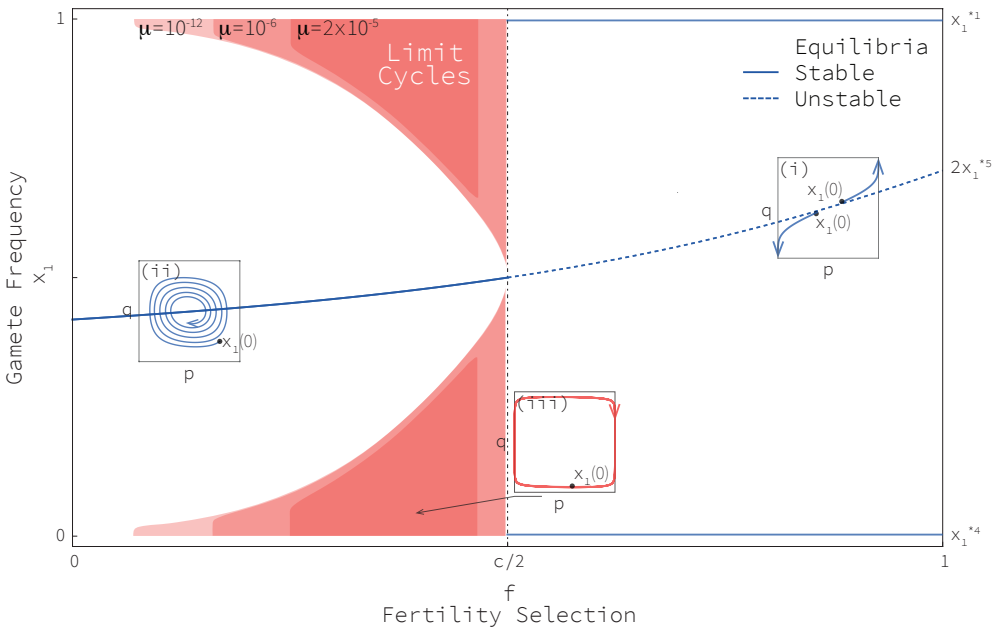

Figure 2: **Basin of attraction of limit cycles and each equilibrium**. This figure depicts the frequency of gametic type A_1B_1 (x_1) as a function of the fitness cost f for given values of r_m, b, c, μ. When $f > \frac{1}{2}c$ and $\mu > 0$ equilibria $\mathbf{x}^{*\mathbf{1}}, \mathbf{x}^{*\mathbf{4}}, \mathbf{x}^{*\mathbf{5}}$ are biologically meaningful. Equilibria $\mathbf{x}^{*\mathbf{1}}$, $\mathbf{x}^{*\mathbf{4}}$ are stable whereas equilibrium $\mathbf{x}^{*\mathbf{5}}$ is unstable. The figure is constructed by starting trajectories at different initial conditions, sampled at equally spaced intervals along the line connecting corners $(1, 0, 0, 0)$ and $(0, 0, 0, 1)$ for which $(x_1(0), x_2(0), x_3(0), x_4(0)) = (x_1(0), 0, 0, 1 - x_1(0))$. Initial conditions above the dotted curve (which represents equilibrium $\mathbf{x}^{*\mathbf{5}}$) lead to equilibrium $\mathbf{x}^{*\mathbf{1}}$ while those below $\mathbf{x}^{*\mathbf{5}}$ lead to $\mathbf{x}^{*\mathbf{4}}$. This behaviour is summarised using inset (i), which represents the dynamics in the allelic space (p, q). When $f < \frac{1}{2}c$ and $\mu > 0$, only equilibrium $\mathbf{x}^{*\mathbf{5}}$ is inside the region where x_1 has biological meaning. Equilibrium $\mathbf{x}^{*\mathbf{5}}$ is stable. Trajectories starting at initial condition $x_1(0)$ within the white region spiral towards the symmetric internal equilibrium (see inset ii). When initial conditions are within the red region, the solutions oscillate towards a limit cycle (see inset iii). As the mutation probability increases, the set of initial conditions converging to the stable limit cycle shrinks.

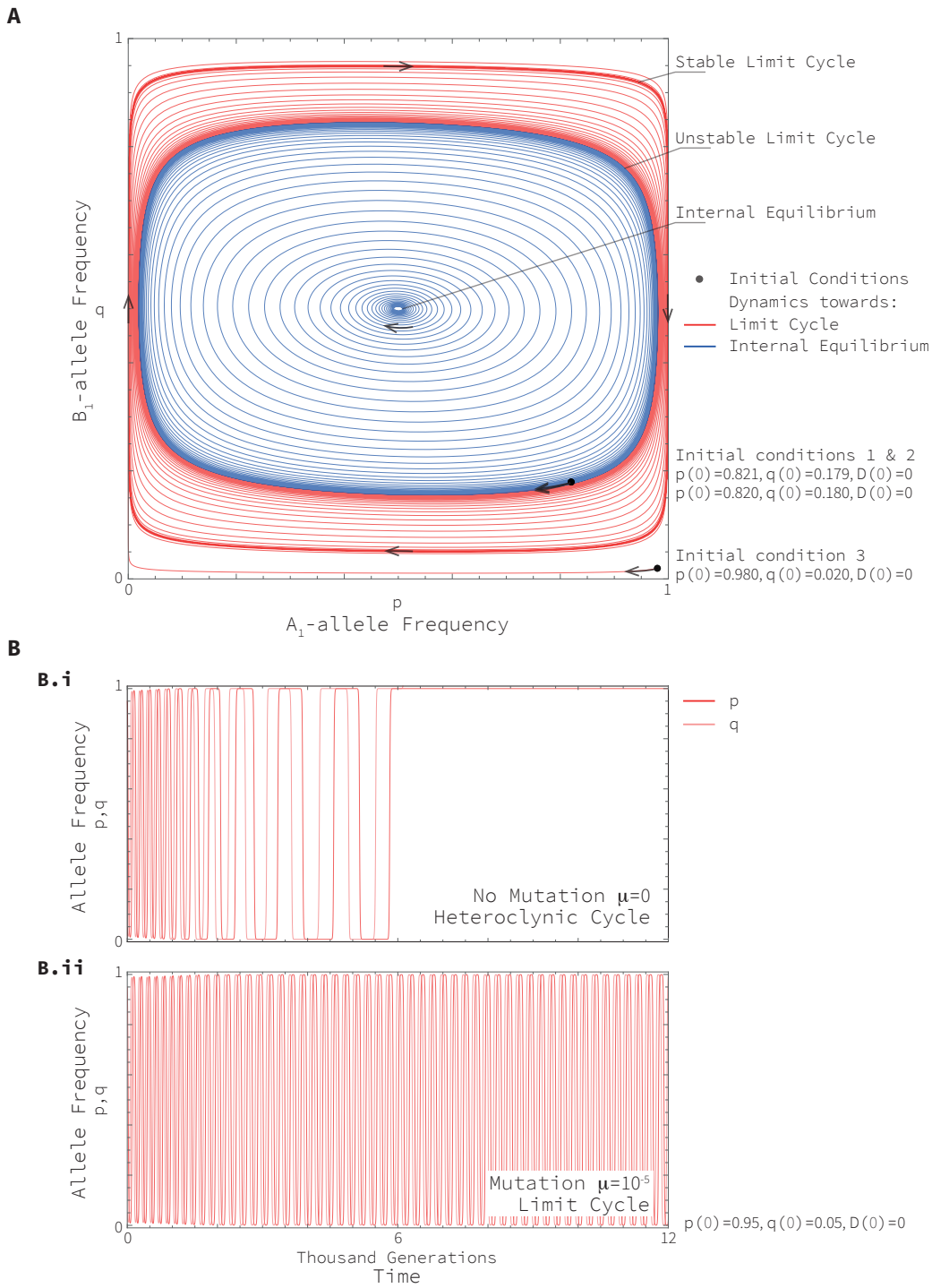

Figure 3: **Examples of dynamics of the allelic frequencies in the parameter region $f < \frac{1}{2}c$. Panel A** displays the dynamics in (p, q)-space. It shows the existence of a stable limit cycle, an internal equilibrium and an unstable limit cycle separating them. Red and blue are used to represent the trajectories leading to the stable limit cycle and the internal equilibrium respectively. The trajectories correspond to the set of parameter values $f = 0.4$, $b = c = 1$, $r_m = \frac{1}{2}$, $\mu = 10^{-5}$. **Panel B** displays the frequencies of p and q as a function of time. **Subpanel B.i** provides an example when there is no mutation, $\mu = \mu_A = \mu_B = 0$. **Subpanel B.ii** provides an example when there is mutation, $\mu = \mu_A = \mu_B = 10^{-5}$. Both trajectories correspond to the set of parameter values $f = 0.26$, $b = 1$, $c = r_m = \frac{1}{2}$.

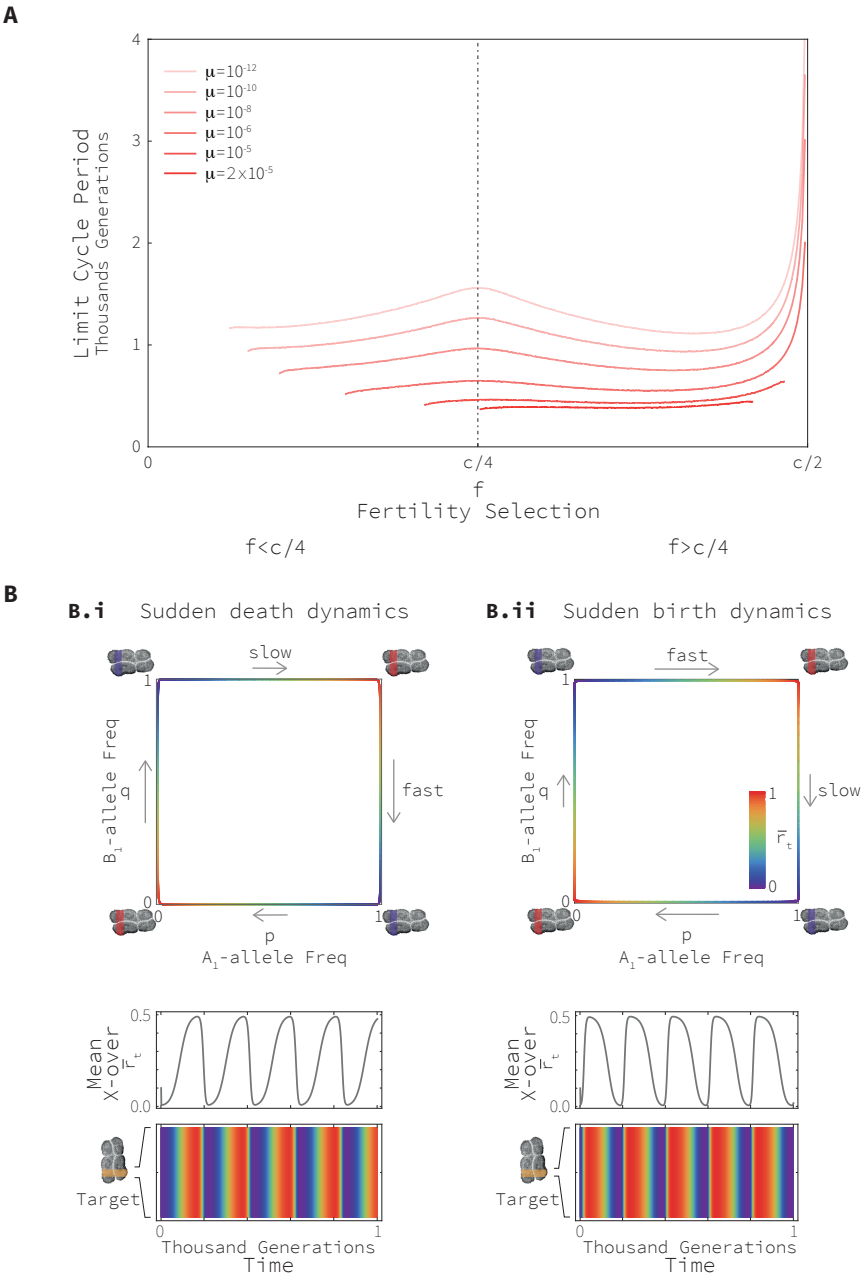

Figure 4: **Periodicity of limit cycles. Panel A** displays the period of limit cycles as a function of the fitness cost f within the parameter region $(0, \frac{1}{2}c)$. Results are illustrated for different mutation rates $\mu = \mu_A = \mu_B$. The parameter values used to create this figure are $b = c = 1$, $r_m = \frac{1}{2}$. Initial conditions are $(x_1(0), x_2(0), x_3(0), x_4(0)) = (a, 0, 0, 1-a)$ where $a = 0.005$). **Panel B** displays the genetic and phenotypic oscillations over time. **Sub-panel B.i** displays the case when $0 < f < \frac{1}{4}c$. Here the transition from hot to cold is faster than the transition from cold to hot. We refer to this type of dynamics as "sudden death dynamics". To create this panel we assumed $f = 0.1$. **Sub-panel B.ii** displays the case when $\frac{1}{4}c < f < \frac{1}{2}c$. Here the transition from cold to hot is faster than the transition from hot to cold. We refer to this type of dynamics as "sudden birth dynamics". To create this panel we assumed $f = 0.4$. Within each sub-panel there are three figures: The first one depicts the change in allele frequencies in the limit cycle. The second and third figures depict the change in crossover probability at the target locus over time. Heat maps (third figures) are designed so that red colours correspond to high crossover probabilities (hotspot), and blue colours correspond to low crossover probabilities (coldspot). In Panel B we assumed that $b = c = 1$, $r_m = \frac{1}{2}$, $\mu = 10^{-9}$, and $p(0) = 0.99$, $q(0) = 0.01$, $D(0) = 0$.

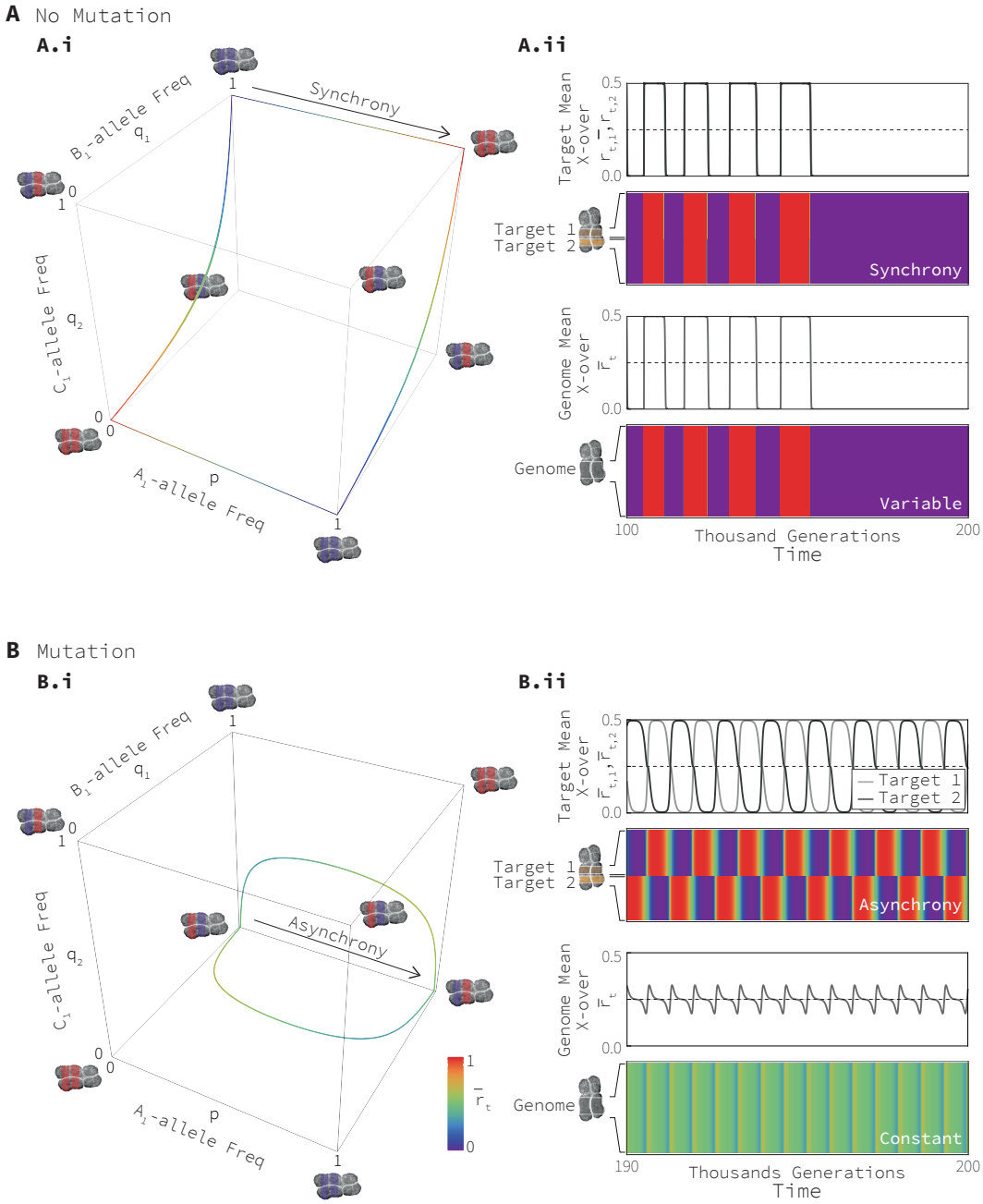

Figure 5: **Genetic and phenotypic variation over time in a system with two targets.** Cubes represent the change in allele frequency in PRDM9 and target loci. Figures depict the average recombination in each of the target sites and the genome (meaning the average across all targets). These are represented both as lines and heat maps. **Panel A** corresponds to the case where there are no mutations ($\mu_A = \mu_B = \mu_C = 0$). **Sub-panel A.ii** shows that the dynamics converge to heteroclynic cycles such that both target loci are hot or cold at the same time (synchronic oscillation) and the average genome recombination is variable (oscillating with the average recombination in each target). **Panel B** corresponds to the case where there are mutations (in particular $\mu_A = 10^{-8}$, and $\mu_B = \mu_C = 10^{-6}$). **Sub-panel B.ii** shows that the dynamics converge to limit cycles such that one target is hot when the other is cold or vice-versa (asynchronic oscillation) and the average genome recombination is close to being constant (showing minimal oscillation). Here we assumed that $f = 0.18$, $b = 1$, $c = r_m = \frac{1}{2}$, and $p(0) = q_1(0) = 0.9$, $q_2(0) = 0.8$, $D(0) = 0$.

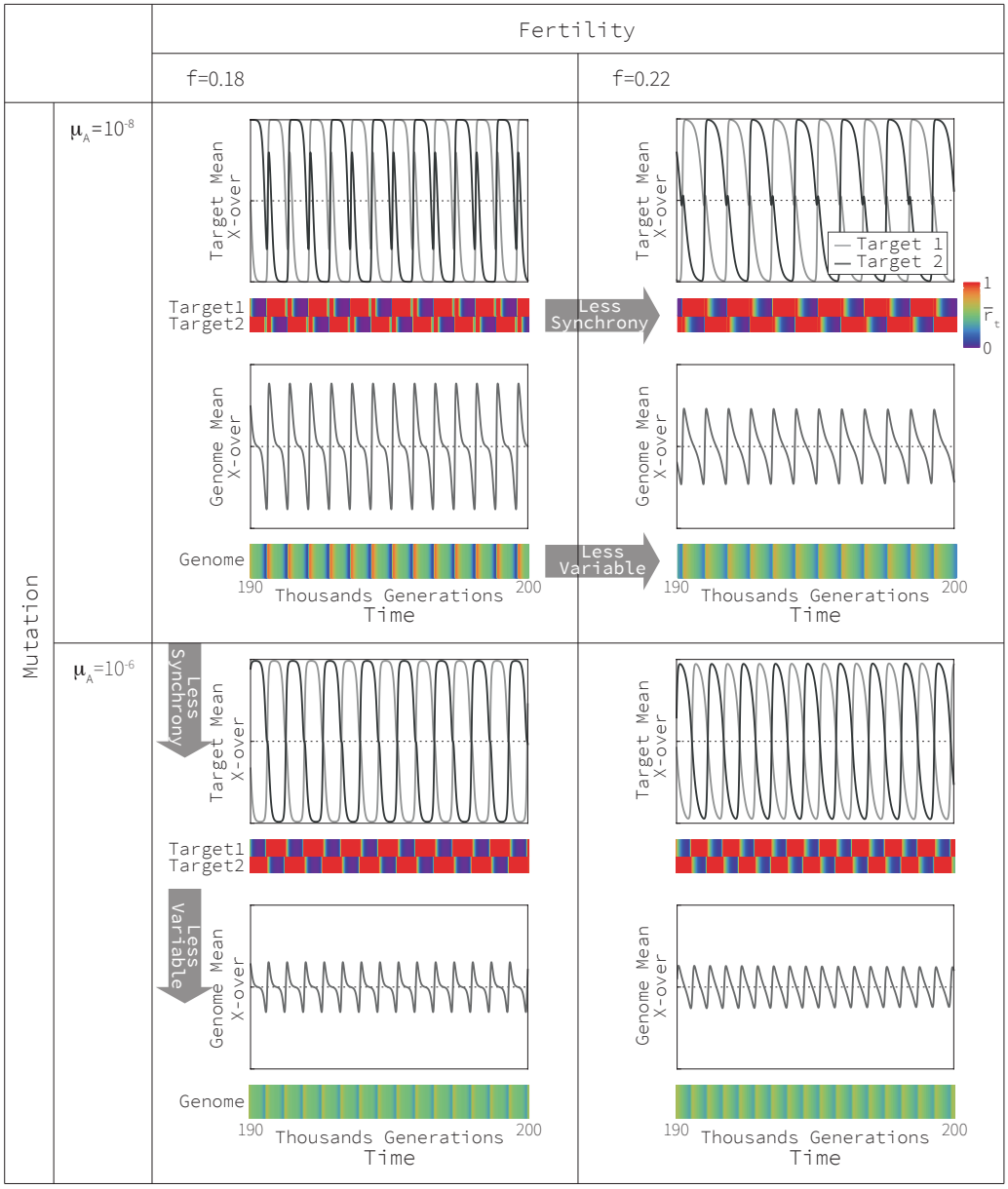

Figure 6: **Effect of mutation probability and selection on the asynchrony of oscillations in each target.** This figure depicts the change in crossover probability at each of two target loci for different combinations of the mutation probability and fertility selection, along with the genome-wide mean crossover probability. This figure shows that the greater the mutation probability the lower the overlap of hot and cold phenotypes at different target loci (the greater the asynchrony) and the lower the oscillation of the genome mean crossover probability. Notice that mutation does not affect the amplitude of the oscillation in each target. Here we assumed $b = 1$, $c = r_m = \frac{1}{2}$, and initial frequencies of: $p(0) = q_1(0) = 0.9$, $q_2(0) = 0.8$, $D(0) = 0$.

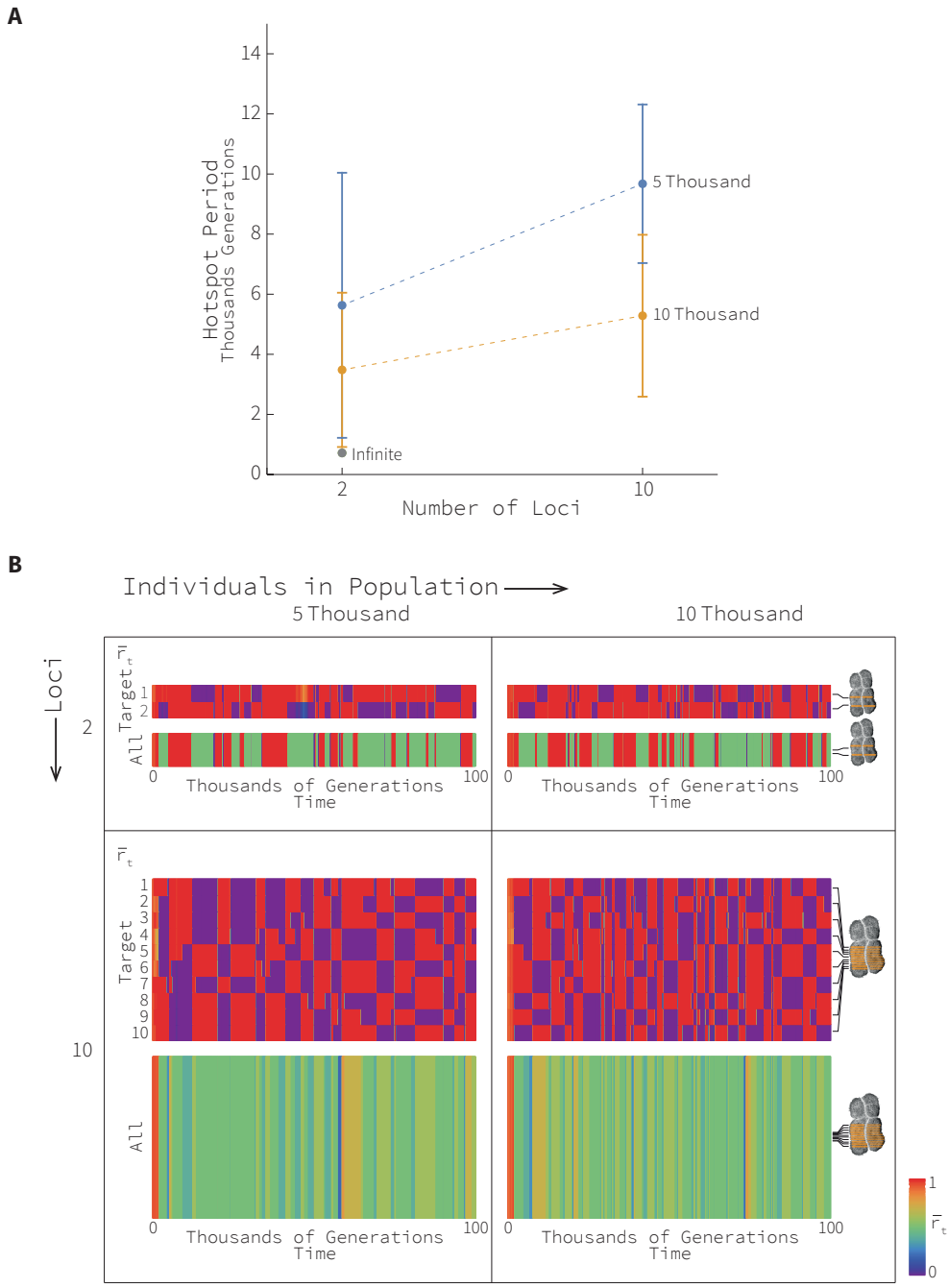

Figure 7: **Effect of population sizes and number of targets on the speed of hotspot oscillations in finite populations. Panel A** shows the average period of an oscillation between hot and cold states. Blue and orange dots represent the average value of the period (for two targets in 100 thousand generations) when the population size is five and ten thousand individuals respectively. The grey dot represents the equivalent value for an infinite population. Vertical bars correspond to the standard deviation. We make the conservative assumption that there is only one attempt to produce one double strand break per genome per generation. **Panel B** shows examples of dynamics. Examples are arranged in a table with five and ten thousand individuals in the columns and two and ten loci in the rows. This figure shows that the smaller the population size or the greater the number of target loci the greater the period of hotspot oscillations. Here we assumed that $f = 0.4$, $b = c = 1$, $r_m = \frac{1}{2}$ (the recombination rate between any pair of loci is also $\frac{1}{2}$), $\mu_A = 10^{-6}, \mu_B = 10^{-7}$, and $p(0) = 0.95$, $q(0) = 0.95$, $D(0) = 0$.

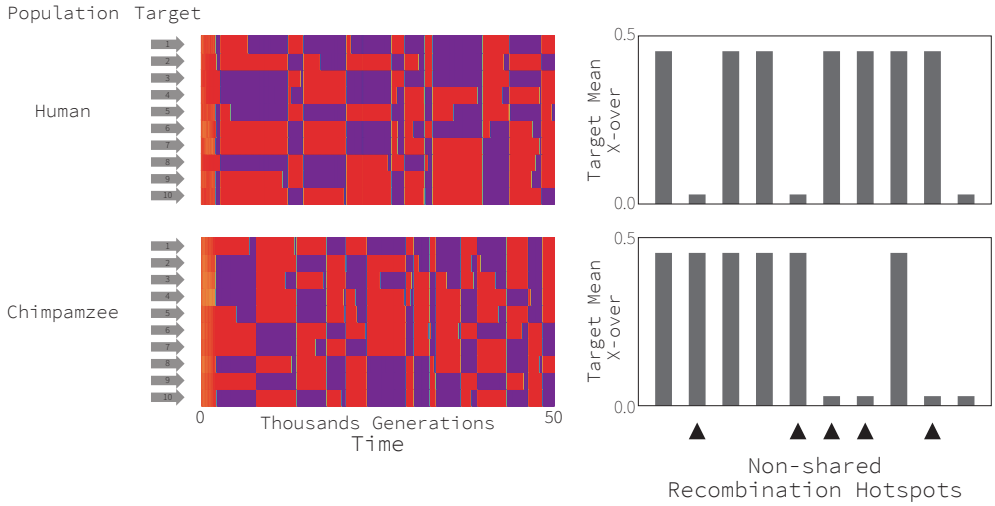

Figure 8: **Evolution of the recombination landscape in two separate populations when hotspots resuscitate** This figure shows the hotspots that are shared and non-shared between these two populations after 10 thousand generations. Here we assume that $b = c = 1$, $r_m = \frac{1}{2}$ (the recombination rate between any pair of loci is also $\frac{1}{2}$), $\mu_A = 10^{-6}, \mu_B = 10^{-7}$, and $p(0) = 0.95$, $q(0) = 0.95$, $D(0) = 0$.